Published OnlineFirst August 29, 2012; DOI: 10.1158/0008-5472.CAN-12-1470

Integrated Systems and Technologies

Cancer Research

Ploidy and Large-Scale Genomic Instability Consistently Identify Basal-like Breast Carcinomas with *BRCA1/2* Inactivation

Tatiana Popova[1,2], Elodie Manié[1,2], Guillaume Rieunier[1,2], Virginie Caux-Moncoutier[3], Carole Tirapo[3], Thierry Dubois[1,4], Olivier Delattre[1,2], Brigitte Sigal-Zafrani[3], Marc Bollet[5], Michel Longy[7], Claude Houdayer[3,6], Xavier Sastre-Garau[3], Anne Vincent-Salomon[1,2,3], Dominique Stoppa-Lyonnet[1,2,3,6], and Marc-Henri Stern[1,2,3]

Abstract

BRCA1 inactivation is a frequent event in basal-like breast carcinomas (BLC). However, *BRCA1* can be inactivated by multiple mechanisms and determining its status is not a trivial issue. As an alternate approach, we profiled 65 BLC cases using single-nucleotide polymorphism arrays to define a signature of *BRCA1*-associated genomic instability. Large-scale state transitions (LST), defined as chromosomal break between adjacent regions of at least 10 Mb, were found to be a robust indicator of *BRCA1* status in this setting. Two major ploidy-specific cutoffs in LST distributions were sufficient to distinguish highly rearranged BLCs with 85% of proven *BRCA1*-inactivated cases from less rearranged BLCs devoid of proven *BRCA1*-inactivated cases. The genomic signature we defined was validated in a second independent series of 55 primary BLC cases and 17 BLC-derived tumor cell lines. High numbers of LSTs resembling *BRCA1*-inactivated BLC were observed in 4 primary BLC cases and 2 BLC cell lines that harbored *BRCA2* mutations. Overall, the genomic signature we defined predicted *BRCA1/2* inactivation in BLCs with 100% sensitivity and 90% specificity (97% accuracy). This assay may ease the challenge of selecting patients for genetic testing or recruitment to clinical trials of novel emerging therapies that target DNA repair deficiencies in cancer. *Cancer Res; 72(21); 5454–62. ©2012 AACR.*

Introduction

Basal-like breast carcinomas (BLC) are generally described as high-grade ductal carcinomas with a so-called triple-negative phenotype [absence of estrogen receptor (ER), progesterone receptor (PR), and HER2/ERBB2 overexpression/amplification] and markers expressed by the normal basal/myoepithelial cells of the mammary gland [such as cytokeratins 5/6, 14, 17, and epidermal growth factor receptor (EGFR); for review, see ref. 1]. The BLC entity partially overlaps with the larger triple-negative breast carcinoma (TNBC) disease (1). The breast cancer susceptibility gene *BRCA1* has a particular relationship to the basal-like phenotype. Firstly, BLCs represent the majority of breast carcinomas arising in *BRCA1* mutation carriers, while representing less than 20% of sporadic breast tumors (2). Secondly, the high level of genomic instability observed in BLCs (3–5) fits *BRCA1* involvement in double strand break signaling and repair by homologous recombination (HR; for review, see ref. 6). However, whether so-called BRCAness or HR deficiency is a general feature of BLCs (7) remains controversial, as *BRCA1* inactivation (by mutation or methylation of *BRCA1* promoter) is evidenced in less than 30% of BLC/TNBCs (8), and a high level of genomic instability and response to treatment exploiting HR deficiency are inconsistently found in these tumors (9–12).

Considering its importance in diagnosis and treatment stratification, many studies have tried to define clinically relevant surrogate markers of BRCAness; for review, see ref. 13. Genomic markers of BRCAness were searched for by comparing array-CGH profiles of *BRCA1*-mutated versus unselected hereditary or sporadic breast tumors (14–17). Studies comparing BLCs with or without *BRCA1* inactivation either found no difference (10, 18, 19) or identified 3q gain as associated with *BRCA1* inactivation (11). A classifier based on array-CGH profiles and trained on *BRCA1* mutated tumors within unselected group of tumors (20) showed a sensitivity of approximately 80% in TNBCs in 2 independent studies (21, 22).

The goal of this study was to identify genomic markers predicting actual *BRCA1* inactivation within the group of BLCs. Analysis of single-nucleotide polymorphism (SNP)-array data using a specific data processing method (genome

Authors' Affiliations: [1]Centre de Recherche, [2]INSERM U830, Departments of [3]Tumor Biology, [4]Translational Department, and [5]Radiotherapy, Institut Curie, [6]Sorbonne Paris Cité, University Paris-Descartes, Paris; and [7]Institut Bergonié, Bordeaux, France

Note: Supplementary data for this article are available at Cancer Research Online (http://cancerres.aacrjournals.org/).

T. Popova and E. Manié equally contributed to this work.

Corresponding Author: Marc-Henri Stern, Institut Curie, INSERM Unit 830, 26 rue d'Ulm 75248 PARIS cedex 05, France. Phone: 33-1-562-46646; Fax: 33-1-562-46630; E-mail: marc-henri.stern@curie.fr

doi: 10.1158/0008-5472.CAN-12-1470

Published OnlineFirst August 29, 2012; DOI: 10.1158/0008-5472.CAN-12-1470

alteration print, GAP; ref. 23) identified ploidy and large-scale chromosomal breaks to be strongly predictive of the *BRCA1* inactivation regardless of the mechanism of inactivation. Moreover, *BRCA2* appeared mutated in a significant number of BLCs displaying similar features to *BRCA1* inactivated cases, supporting the efficiency of these genomic markers in predicting the actual *BRCA1* and *BRCA2* status of these tumors.

Patients and Methods

Patients and tumors

The experimental series consisted of 80 undifferentiated BLCs from patients treated by first-line surgery at the Institut Curie [some BLCs have been described previously: GEO GSE18799 (23–26)]. All tumors were negative for ER, PR [<1% nuclear staining by immunohistochemistry (IHC)], and ERBB2/HER2 [<2+ by IHC or non-amplified by fluorescent *in situ* hybridization]; and positive for either KRT5/6/14/17 or EGFR by IHC (24, 25). Tumor DNA and RNA extracted from frozen tissue were obtained from the Institut Curie Biological Resource Center. This series comprised a high proportion of tumors arising in patients carrying a deleterious germline *BRCA1* mutation (31 tumors). The validation series comprised 60 samples with available SNP array profile including BLCs from a cohort of young women (19 cases; ref. 27), BLCs (15 cases) including 1 case with *BRCA2* germline mutation, all from Institut Curie (34 cases; Affymetrix SNPchip6.0); *BRCA1* BLCs from GEO GSE19177 (12 cases; Illumina 370K; ref. 18); BLCs from GEO GSE32530 (5 cases and their xenografts; Affymetrix SNPchip6.0; ref. 28); and *BRCA1* BLCs from Institut Bergonié (9 cases; Illumina 660K).

This research was approved by the institutional review boards of the Institut Curie. According to French regulations, patients were informed of the research conducted using the biologic specimens obtained during their treatment and did not express opposition. Germline *BRCA1/2* gene analyses were conducted exclusively in patients who attended a visit with a geneticist and a genetic counselor in a family cancer clinic, mostly at the Institut Curie, Paris, France and after informed consent.

Cell lines

The SNP array profiles were available for 17 basal-like cell lines [13 cell lines from American Type Culture Collection (ATCC) and BC227 cell line derived from HBCx-17 tumorgraft; ref. 29], hybridized at Institut Curie; HCC1395, HCC70, and MDA-MB-435 data obtained from the Wellcome Trust Sanger Institute Cancer Genome Project (30). The cell line series included HCC1395, MDA-MB-436, and HCC1937 bearing *BRCA1* mutations (31, 32), HCC38 with *BRCA1* promoter methylation (33), BC227, and HCC1599 with *BRCA2* c.6033_6034delTT/p.S2012QfsX5, and c.4550_4559del10/p.K1517IfsX23 mutations, respectively [the HCC1599 mutation described in catalogue of somatic mutations in cancer (COSMIC; ref. 34) and verified by Sanger sequencing]. Deep sequencing data for the 5 triple negative cell lines and corresponding SNP arrays were retrieved from the Supplementary materials of Stephens and colleagues (31).

Validation of cell lines. Breast cancer cell lines were purchased in May 2006 and May 2008 from ATCC, routinely cultured as recommended by manufacturer and used from passages 3 to 13 before analysis by SNP array. Authentification of the cell lines was conducted from the same passage than one used for experiments by verifying by Sanger sequencing the published *TP53* (HCC38, HCC1143, and MDA-MB-468), *BRCA1* (HCC1937 and MDA-MB-436), and *BRCA2* (BC227 and HCC1599) mutations.

Methylation status of the *BRCA1* promoter

Methylation of the *BRCA1* promoter was assessed by methyl-specific PCR after bisulfite conversion using the MethylDetector Kit (Active Motif), as described previously (24), with minor modifications (primer sequences are available upon request).

BRCA1 mutation status

Prescreen for mutations of the *BRCA1/2* gene was conducted using Enhanced Mismatch Mutation Analysis [EMMA, Fluigent (35); EMMALYS software P/N: 5331254102]. For abnormal EMMA profiles, the *BRCA1/2* exons concerned were sequenced with dideoxynucleotides (BigDye Terminator V1.1, Seqscape V2.5, Applied Biosystems) according to standard protocols (primer sequences and protocols are available upon request).

Translocation-specific PCR

Primers were designed to validate chromosomal translocations in tumor DNA from case BLC_B1_T06 (T1 from ref. 36) by translocation specific PCR. Primers and PCR program are available upon request.

Detection of RAD51 foci by immunofluorescence after ionizing radiation

Breast cancer cell lines were irradiated with a dose of 10 Grays (Gy) using a Cesium gamma-irradiator IBL137 (1.73 Gy/min for 345 s) and incubated at 37°C for 8 hours. After fixation with 4% paraformaldehyde and permeabilization with 0.1% sodium dodecyl sulfate, cells were incubated with anti-RAD51 (Abcam), and anti-53BP1 (Novus Biologicals) and then with anti-mouse Alexa Fluor 488 and anti-rabbit Alex Fluor 555 (Molecular Probes), respectively. Images were acquired using a Zeiss Axioplan 2 fluorescence microscope with a 100X/1.3 oil immersion objective, in 8-bit format and analyzed with ImageJ software (37). Images were then converted in 8-bit format for the final figures. Space resolution is 0.129 μm × 0.129 μm (*xy*). Scale bars, 20 μm.

SNP arrays

Genomic profiling was conducted using 2 platforms: Illumina (32 cases; Human Hap300-Duo) and Affymetrix (48 cases; SNPChip6.0 array). Hybridization on the Illumina platform was conducted by a service provider (Integragen); raw data files were processed by BeadStudio 3.3 (Illumina, reference model file HumanHap300v2_A); normalization was conducted using the tQN algorithm (38). Hybridization on Affymetrix platform was conducted at Institut Curie; cell files were processed by Genotyping Console 3.0.2 (Affymetrix, reference model file HapMap270, version 29).

Published OnlineFirst August 29, 2012; DOI: 10.1158/0008-5472.CAN-12-1470

Processing SNP arrays. Both Illumina and Affymetrix SNP array data were mined using the previously described and validated GAP method (23). *R* scripts and full details of the application are available at the web site. Recognition of absolute copy number ranged from 0 to 8 copies and all segments exceeding 8-copy level were ascribed 8-copy status. Twenty-two possible segmental genotypes were therefore discriminated: A (1 copy); AA and AB (2 copies); AAA and AAB (3 copies); AAAA, AAAB, and AABB (4 copies); etc.

Chromosome number was estimated by the sum of the copy numbers detected at the pericentric regions (with an error rate less than 2 chromosomes per genome as assessed in 25 cell lines with known karyotype, see Supplementary Table S1).

Number of breakpoints in each genomic profile was estimated based on the resulting interpretable copy number profile and after filtering smaller than 50 SNPs variations.

Results

BRCA1 status of basal-like breast carcinomas

High-quality SNP arrays were obtained for 65 BLCs (15 of the 80 SNP arrays were discarded because of low hybridization quality, low tumor content, or ambiguous profile interpretation), including 23 tumors from patients carrying deleterious *BRCA1* mutations (hereafter called *BRCA1* BLCs) and 42 BLCs from patients with no evidence of familial predisposition of breast/ovarian cancer or tested negative for *BRCA1/2* mutations (hereafter called sporadic BLCs). Forty-one of the 42 sporadic BLCs were tested for methylation of the *BRCA1* promoter and nearly 25% were found positive (11/41, hereafter called *meBRCA1* BLCs; ref. 24). No evidence of methylation was observed in the remaining 31 cases (hereafter called non-*BRCA1* BLCs). *BRCA1* epigenetic status was consistent with *BRCA1* expression in all 37 cases tested with available transcriptomic data. *BRCA1* and *meBRCA1* BLCs comprised the group of tumors with proven *BRCA1* inactivation (34 cases) that were further compared with the group of presumably non-*BRCA1* BLCs (31 cases). Loss of heterozygosity at the *BRCA1* locus was observed in 61 BLCs, including all *BRCA1* and *meBRCA1* BLCs. As previously described, 95% of the evaluated cases were found mutated for *TP53* (41/43 BLCs; the 2 *TP53* wild-type cases were *BRCA1* BLCs; ref. 24).

Near-diploidy in BLCs has a high positive predictive value for *BRCA1* inactivation

To obtain insight into the specific genomic alterations of BLCs, genomic profiling was conducted using SNP arrays, which provide 2 complementary measurements: copy number variation and allelic imbalance. The GAP methodology for mining SNP arrays (23) provided segmental genotype profiles (i.e., absolute copy numbers and allelic contents) for each sample (Supplementary Fig. S1). General genomic characteristics, such as chromosome number, DNA index, number of chromosome breaks, and proportions of genome in each genomic state, were inferred from the segmental genotype profiles.

Inferred chromosome counts per genome showed a bimodal distribution (Fig. 1A) similar to those showed for the genomes in various types of cancers (39). Tumor genomes carrying less than 50 chromosomes with a DNA index close to 1 were considered to have a "near-diploid" genome. On the basis of the hypothesis of duplication of the whole genome during cancer progression explaining the second mode of chromosome distribution (39), tumor genomes carrying more than 50 chromosomes and a DNA index higher than 1.2 were considered to have a ploidy of 4 and are hereafter called "near-tetraploid genomes." More detailed considerations of the genomic alteration patterns justified the ploidy attribution and revealed 1 outlying case to be considered as near-diploid despite the detection of more than 50 chromosomes in its genome (Supplementary Table S2 and Fig. S2). Finally, 24 and 41 BLCs were classified as near-diploid and near-tetraploid, respectively.

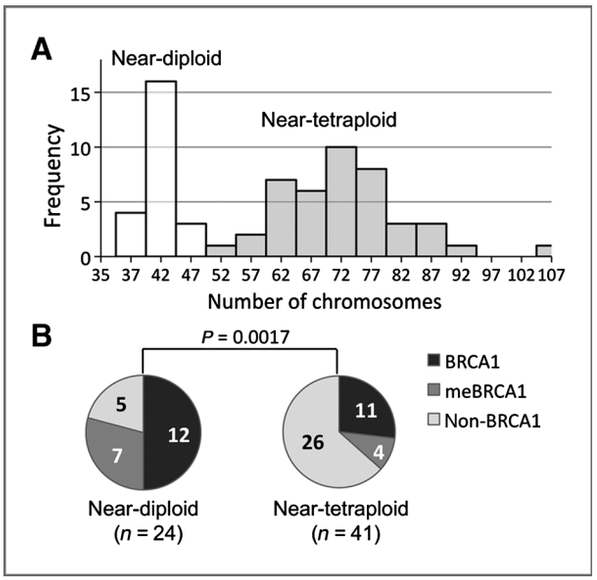

Figure 1. Chromosome content and *BRCA1* status in BLCs. A, distribution of chromosome number in BLCs displayed 2 modes representing 2 ploidy status of tumor genomes. B, near-diploid tumors (<50 chromosomes) and near-tetraploid tumors (≥50 chromosomes) showed different proportions of proven *BRCA1*–inactivated tumors; number of cases are indicated in the circle diagrams.

Interestingly, the near-diploid tumors almost consistently carried germline mutations or epigenetic inactivation of *BRCA1* (19/24) in contrast to the near-tetraploid tumors, which presented a higher proportion of non-*BRCA1* BLCs (26/41; $P < 0.002$; Fig. 1B). Therefore, in our series of tumors, a near-diploid status had 80% [95% confidence interval (CI), 64%–96%] positive predictive value for *BRCA1* inactivation.

Large-scale chromosomal rearrangements discriminate *BRCA1* and non-*BRCA1* basal-like carcinomas

The total number of breakpoints detected in a cancer genome characterizes the level of genomic instability (40). Overall comparison of *BRCA1* versus non-*BRCA1* tumors did not show any significant difference ($P = .13$). In the subgroup of 41 near-tetraploid BLCs, 15 *BRCA1*-inactivated tumors displayed an elevated total number of breakpoints (199 ± 72; range: 85–294), whereas 26 non-*BRCA1* tumors were more

Published OnlineFirst August 29, 2012; DOI: 10.1158/0008-5472.CAN-12-1470

heterogeneous (151 ± 67; range: 43–289) and presented a higher proportion of low values compared with *BRCA1* tumors ($P < 0.03$, Wilcoxon rank test). However, the large overlap in breakpoint numbers precluded their direct application to tumor classification.

Recent advances in deciphering tumor genome complexity revealed various mechanisms of alterations associated with different sizes of genomic fragmentation (31, 41, 42), including specific patterns of *BRCA1/2* mutated breast tumors (10). To determine the effective sizes of genomic alterations in BLCs (i.e., the actual distance between 2 adjacent breakpoints) the distribution of segments with the respect to their size was considered. Proportion of segments of a given size, averaged through the 65 BLCs of the experimental cohort, followed a log-linear decay starting from approximately 3 Mb (Fig. 2A, Supplementary Fig. S3). The decreasing rate for the fragments 0–3 Mb displayed a steeper decay, evidencing at least 2 populations of breaks affecting the tumor genome with the prominent cutoff at approximately 3 Mb.

Filtering and smoothing all variations less than 3 Mb resulted in a number of breakpoints more significantly associated with *BRCA1* status than total breakpoint numbers ($P < 0.006$, Wilcoxon rank test in the subgroup of near-tetraploid BLCs, 81.3 ± 20.7 and 54.1 ± 30.1 breakpoints in *BRCA1* and non-*BRCA1* tumors, respectively). We then defined a state transition of the size S Mb if 2 adjacent chromosomal segments, each not less than S Mb in size, have different copy numbers and/or allelic contents. The number of state transitions in the tumor genomes displayed an approximately log-linear decay as a function of S ($S = 3,\ldots,20$ Mb; Fig. 2B). When the segment size S spanned 6 to 11 Mb, near-tetraploid BLCs were split into 2 stable subgroups. The subgroup with the high numbers of state transitions was enriched in *BRCA1* deficient BLCs (16/24), whereas the subgroup with the low numbers of state transitions did not contain any *BRCA1* tumor (0/17) with the most significant difference in mean values observed at $S = 10$ Mb (Fig. 2B and C).

On the basis of these considerations, a large-scale state transition (LST) was defined as a chromosomal break between adjacent regions of at least 10 Mb; the number of LSTs in the tumor genome was estimated for each chromosome arm independently (not accounting for the centromeric breaks) and after filtering and smoothing of all variations less than 3 Mb (Fig. 2D). For the near-tetraploid tumors clear cutoff in

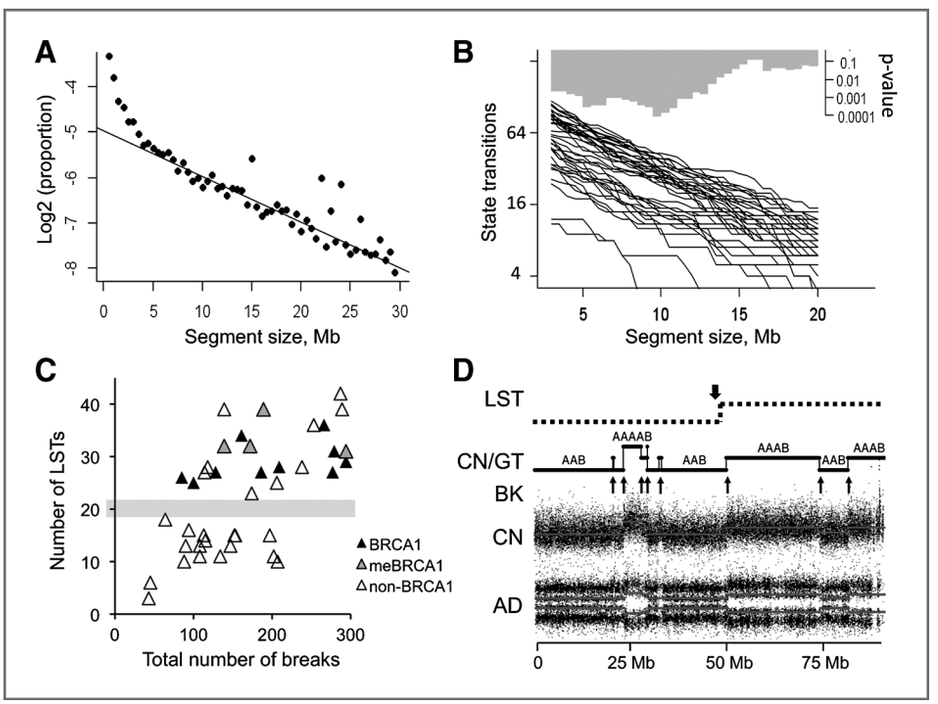

Figure 2. LST number as a surrogate measure of genomic instability A, proportion of segments equal or greater than a given segment size, averaged for the series of 65 BLCs. A linear model was fitted starting from 4 Mb segment size and excluding outliers (values at 15, 22, and 24 Mb were more frequent because of the size of the 18p, 17p, and 19p chromosome arms, respectively). B, number of state transitions depending on the size of the segments; each line corresponds to a near-tetraploid BLC; significance profile for *BRCA1* versus non-*BRCA1* tumors comparison is shown on the top of the plot. C, genomic instability in near-tetraploid BLCs as estimated by the total number of breaks and by LSTs (segment size 10 Mb). LST number clearly discriminated non-*BRCA1* BLCs from BLCs with proven *BRCA1* inactivation ($P < 0.001$, Wilcoxon test). Total number of breaks was less significantly different between non-*BRCA1* versus *BRCA1* and me*BRCA1* comparison ($P < 0.03$, Wilcoxon test) and was not discriminative. BRCA1, germline *BRCA1* mutation; meBRCA1, *BRCA1* promoter methylation; non-BRCA1, absence of evidence of *BRCA1* inactivation. D, an example of genomic profile with 1 LST detected. CN, copy number profile; AD, allelic difference profile; CN/GT, segmental copy numbers and genotypes recognized by GAP; BK, total breaks; LST, large-scale state transition. The dashed line shows large-scale segments obtained after filtering and smoothing small-scale variations seen in the CN/GT profile.

Published OnlineFirst August 29, 2012; DOI: 10.1158/0008-5472.CAN-12-1470

LSTs counts separated 17 non-*BRCA1* BLCs (12.3 ± 3.7 LSTs) from a group of tumors containing 15 *BRCA1*-inactivated and 9 non-*BRCA1* BLCs (31.4 ± 5.8 LSTs; Figs. 2C and 3). In the near-diploid group mainly containing *BRCA1* tumors (19/24), number of LSTs showed a unimodal distribution (25.3 ± 6.1) with 3 non-*BRCA1* BLCs within 1 standard deviation (24, 28, and 32 LSTs) and 2 non-*BRCA1* BLCs below 2 standard deviations from the mean (1 and 12 LSTs; Fig. 3). Therefore, in each ploidy subgroup the elevated number of LSTs was strongly associated with a *BRCA1* inactivated status in BLCs whereas all tumors with reduced number of LSTs showed no evidence of *BRCA1* inactivation.

Validation and nature of LSTs

SNP arrays provide the linear profiles of genetic alterations and LSTs represented a subset of chromosomal breaks, corresponding mainly to copy number alterations (Supplementary Data). To clarify the actual genomic rearrangements behind LSTs, the SNP-array profile from case BLC_B1_T06 was superimposed with its structural rearrangements identified by next generation sequencing (NGS; ref. 36). This tumor classified as near-diploid showed 34 LSTs. Most of LSTs (28 out of 34) were supported by the structural rearrangements detected by NGS representing 19 interchromosomal translocations, 5 tandem duplications, 3 probable inversions, and 1 deletion (Supplementary Table S4 and Fig. S4). Nine alterations were further validated by the Sanger sequencing (36) and 11 additional alterations by translocation-specific PCRs (Supplementary Fig. S5). The majority of LSTs (~70%) were thus corresponding to interchromosomal translocations. In contrast, the small-scale variation (<2 Mb) was shown to be frequently observed in intrachromosomal rearrangements (31), which is consistent with the segment size of 3 Mb detected here as a threshold for the conventionally small variation and filtered out before calculating LSTs.

The number of LSTs accurately reflected the large-scale patterns of genomic instability in the tumors: all tumors with low LSTs displayed either few chromosomal breaks with a high level of aneuploidy (3 samples) or mostly regional accumulations of breaks (16 samples; see, for example, Supplementary Fig. S7). Average number of LSTs per chromosome arm was 3.1 (3.1 ± 1.0, range 0–6). Thus, LSTs avoid any overestimation of the level of genomic instability because of possible catastrophic events affecting individual chromosomes.

Distribution of LSTs along the genome was associated with increased GC content (0.42 vs. 0.399, $P < 10^{-16}$) and gene-rich regions (OR, 1.31; 95% CI, 1.25–1.37; $P < 10^{-16}$). Only 1 of 11 genomic regions with high incidence of LSTs corresponded to a common fragile site (FRA2H; ref. 43; Supplementary Fig. S8).

A 2-step decision rule consistently detects BRCAness in BLCs

On the basis of the structural genomic features of BLCs described above, a 2-step decision rule for *BRCA1*-inactivated tumor selection was constructed. The first step consisted in segregating tumors according to their ploidy (into near-diploid or near-tetraploid); the second step consisted in segregating tumors according to the number of LSTs (into LST^{Hi} or LST^{Low}) using ploidy-specific cutoffs: 15 and 20 LSTs per genome in near-diploid and near-tetraploid cases, respectively. LSTs

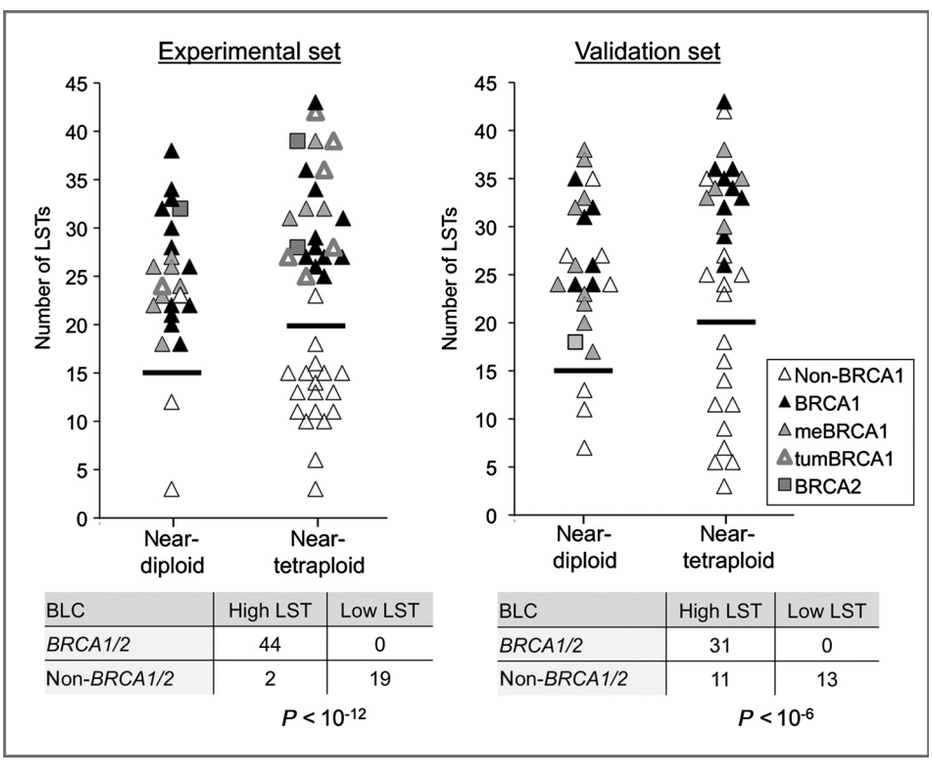

BLC	High LST	Low LST
BRCA1/2	44	0
Non-*BRCA1/2*	2	19

$P < 10^{-12}$

BLC	High LST	Low LST
BRCA1/2	31	0
Non-*BRCA1/2*	11	13

$P < 10^{-6}$

Figure 3. Ploidy and large-scale instability in BLCs. Tumor ploidy and the number of LST are discriminative of *BRCA1/2* inactivation in the experimental (left) and validation (right) sets. Top: number of LSTs per tumor is indicated in relation to ploidy categories. Near-diploid and near-tetraploid cutoffs are indicated by the horizontal bars. Known *BRCA1* and *BRCA2* statuses are indicated for germline mutations (BRCA1 and BRCA2), methylation of the *BRCA1* promoter (meBRCA1) and mutations found in the tumors (tumBRCA1 and BRCA2). Tumors without evidence of *BRCA1/2* inactivation are referred to as non-*BRCA1/2*. Fisher exact tests are indicated below the contingency tables; *BRCA1/2* refers to all proven *BRCA1/2*-inactivated BLCs; non-*BRCA1/2* refers to BLCs without evidence of *BRCA1* or *BRCA2* inactivation.

Published OnlineFirst August 29, 2012; DOI: 10.1158/0008-5472.CAN-12-1470

exceeding the ploidy-specific cutoff identified *BRCA1* deficient tumors with 100% sensitivity and 60% specificity in the experimental set of BLCs ($P < 10^{-3}$, Fisher test; Supplementary Table S4). However, the 12 "false-positive" LST^{Hi} cases may actually have presented *BRCA1* inactivation (not all patients were tested for the germline mutation). The presence of *BRCA1* mutation was investigated in tumor DNA for all cases with available material, including 12 LST^{Hi} BLCs and 15 LST^{Low} BLCs. Deleterious *BRCA1* mutations were found in 7 LST^{Hi} BLCs whereas no mutation was found in LST^{Low} BLC. The somatic origin was shown for 2 of these cases for which germline material and patient consent were available (Supplementary Fig. S9).

The remaining 5 LST^{Hi} BLCs were tested for the *BRCA2* mutation and deleterious mutations were found in 3 cases (Supplementary Data). With these findings, the sensitivity remained unchanged at 100% and the specificity was increased to 90% (including *BRCA1* and *BRCA2* tumors) in the experimental set of BLCs considered (overall accuracy 97%; $P < 10^{-12}$, Fisher test; Fig. 3).

A validation series of 55 BLC/TNBC (5 of the 60 samples were discarded because of low SNP array quality) included 15 cases with a *BRCA1* germline mutation, 15 cases with *BRCA1* promoter methylation, 1 case with a *BRCA2* germline mutation, and 24 presumably non-*BRCA1* cases. SNP array data were processed using the same workflow and structural genomic features were found globally similar to the experimental set (Fig. 3, Supplementary Table S5). Prediction of the *BRCA1* inactivation displayed 100% sensitivity (all 30 *BRCA1* and 1 *BRCA2* inactivated cases were LST^{Hi}) and 54% specificity (11 LST^{Hi} cases were not annotated as *BRCA1/2* inactivated, but no further screening was conducted at the tumor DNA level; $P < 10^{-5}$, Fisher test).

High LSTs consistently predicts BRCAness in basal-like cell lines

A series of 17 basal-like cell lines was analyzed, including 4 cases with *BRCA1* inactivation and 2 cases with *BRCA2* mutations. The results obtained followed the trend observed in primary tumors: firstly, the only near-diploid cell line was the *BRCA1*-mutated MDA-MB-436 (LST^{Hi}); secondly, among near-tetraploid cell lines, HCC1395, HCC1937, HCC38, HCC1599, and BC227 carried the highest number of LSTs, which is again consistent with their *BRCA1/2*-inactivated status (Fig. 4A).

To test functionality of the HR pathway in the basal-like cell lines, formation of RAD51 foci was analyzed after ionizing radiation in 7 cell lines as a read-out of HR pathway proficiency. As expected, no *foci* were observed in the 4 *BRCA1*-deficient cell lines. Interestingly, the 2 assessed LST^{Low} cell lines displayed RAD51 foci accumulation, excluding undetected genetic or epigenetic *BRCA1/2* inactivation in these cell lines (Fig. 4B).

To estimate the stability of LSTs over time and replication, we compared SNP array profiles of primary breast tumors and their xenograft models, at early and late passages when available (28). Number of LSTs displayed high intratumor stability, showing the LST number is an intrinsic property of the tumor, although with some variation with passages (Supplementary Table S7 and Fig. S10).

Discussion

In this study, we addressed prediction of *BRCA1*-inactivated status based on genomic features in the basal-like subtype of invasive ductal breast carcinomas. Analysis of SNP array genomic profiles (23) of well-characterized sets of BLCs identified 2 markers, tumor ploidy, and number of LSTs, which discriminated *BRCA1/2*-inactivated cases with high accuracy.

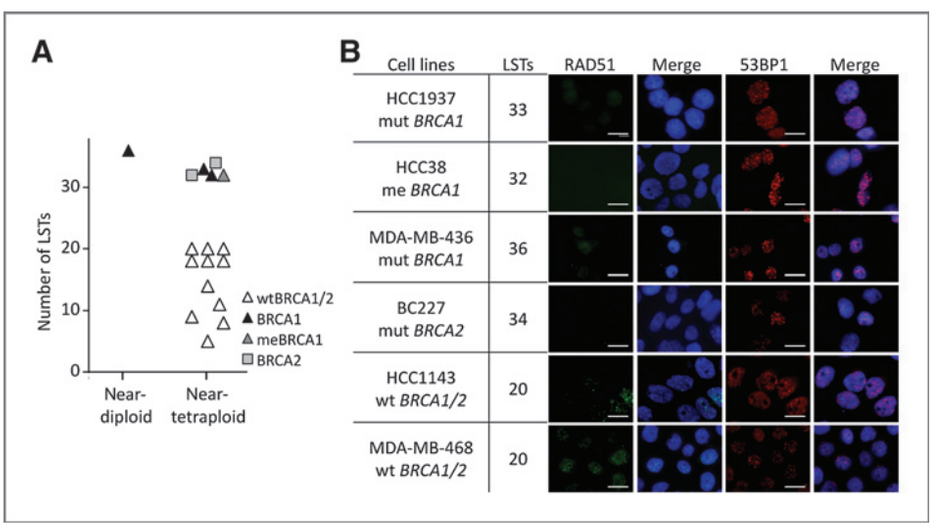

Figure 4. Genomic and functional assessments of BRCAness in basal-like cell lines. A, cell lines with basal-like phenotype display discriminative features of BRCAness similar to primary BLCs. Known status for *BRCA1* and *BRCA2* are indicated for germline mutations (BRCA1 and BRCA2) and methylation of *BRCA1* promoter (meBRCA1). Cell lines without evidence of *BRCA1/2* inactivation are described as wtBRCA1/2. B, RAD51 foci formation 8 hours after 10 Gy irradiation illustrates active HR in non-*BRCA1* cell lines and, conversely, deficient HR in *BRCA1* or *BRCA2* mutated cell lines. 53BP1 foci in the same experiment are shown as a control for DNA damage response. Scale bars, 20 μm. Number of LST is indicated as well as *BRCA1/2* status. mut, mutated; me, methylation of the promoter; wt, wild type.

Published OnlineFirst August 29, 2012; DOI: 10.1158/0008-5472.CAN-12-1470

Our analysis of BLCs genomic profiles provided 2 novel findings. First, tumor genomes with near-diploid and near-tetraploid genomic contents also differed in terms of *BRCA1* status: more than 80% of near-diploid tumor genomes were associated with *BRCA1* inactivation (because of mutation or promoter methylation), whereas non-*BRCA1* tumors had mostly near-tetraploid genomes. Second, the number of LSTs (chromosomal breaks between 2 adjacent regions of at least 10 Mb in size calculated after filtering of all variation less than 3 Mb in size) was introduced as a surrogate measure of a large-scale genomic instability. A prominent cutoff in the LST distribution was observed in each ploidy subgroup that distinguished highly rearranged genomes with a high proportion of proven *BRCA1/2*-inactivated BLCs from discriminatively less rearranged genomes without any proven *BRCA1/2*-inactivated BLCs. The nature of LSTs was clarified by matching them with rearrangements detected by complete genome sequencing of the same sample (36), and 2/3 of the LSTs were found corresponding to interchromosomal translocations.

A decision rule based on the ploidy-specific LST cutoffs correctly predicted all proven *BRCA1*-inactivated tumors in 2 independent series of BLCs (100% sensitivity). The discriminative power of LSTs was further reinforced by deleterious *BRCA1* and *BRCA2* mutations found in 10 of 12 LST^{Hi} BLCs tested with no previous evidence of *BRCA1* inactivation, whereas no mutation was detected in the LST^{Low} BLCs tested (90% specificity). Two *BRCA1* mutations were confirmed to be of somatic origin, further supporting the role of *BRCA1* somatic mutations in breast carcinomas (8).

Inactivation of *BRCA2* in 6 LST^{Hi} samples (4 primary tumors and 2 cell lines) suggested that a high level of LST may be a marker of HR pathway deficiency more than a marker of *BRCA1* status alone. According to this hypothesis, inactivation of other gene products involved in the HR pathway, such as PALB2/FANCN, BRIP1/FANCJ, or RAD51 paralogs, could potentially explain some of the non-*BRCA1/2* LST^{Hi} cases (6).

The greater instability in *BRCA1/2*-associated BLCs showed in our study is in line with the observation based on array-CGH (11) showing a lower mean number of breaks in high *BRCA1*-expressing BLCs compared with low *BRCA1*-expressing BLCs. It was also observed that *BRCA1* and *BRCA2* deficient tumors acquired copy number alterations in longer DNA segments (10). However, estimation of genomic instability using SNP arrays presents a number of advantages over array-CGH. First, the 2 complementary profiles provided by SNP arrays (copy number and allelic difference) give a more robust estimation of breakpoint number. Second, SNP array analyses can be used to infer chromosome numbers and tumor ploidy status (23, 44). On the other hand, using large-scale chromosome breaks to characterize genomic instability is largely independent of SNP array resolution, sample quality, stromal cell contamination, and segmentation algorithm.

SNP arrays provide the linear profile of genetic alterations and LSTs represented a subset of chromosomal breaks, largely representing interchromosomal rearrangements. In HR deficiencies, double-strand DNA breaks are thought to be repaired by nonhomologous end joining, a process that may generate translocations (6). This provides a plausible explanation for the increase of LSTs in a *BRCA1/2*-deficient context. The exhaustive characterization of a large number of BLCs using whole genome sequencing with mate-paired strategies will be mandatory to precisely attribute patterns of large-scale instability to *BRCA1/2* status. Until NGS developments make them cost- and time-effective, SNP-array approaches represent a valuable alternative in a clinical setting.

Our findings raise several questions. First, our analysis strongly suggests that BLCs actually include at least 2 different entities, differing in terms of their *BRCA1/2* status. Interestingly, this dichotomy also exists in basal-like cellular models, in complete concordance with *BRCA1/2* status and HR capacity. Further investigations will be required to determine whether these entities also differ in terms of oncogenic pathways. Second, the fact that *BRCA1*-deficient tumors are more frequently diploid than non-*BRCA*1 BLCs is rather intriguing, considering the numerous reports linking BRCA1 to centrosome structure and functions, and experimentally demonstrating aneuploidy and centrosome amplification as a consequence of *BRCA1* inactivation (45). It is possible that near-tetraploid *BRCA1*-inactivated tumors are less frequently viable because of centrosome clustering dysfunction, multipolar division, and cell death in this particular genetic context (46). Alternatively, *BRCA1*-associated BLCs may have less selective advantages to undergo genome duplication than sporadic cases.

Interestingly enough, genomic instability as measured by number of LSTs was similar in triple negative cell lines with a long history of cell division *in vitro* to that in primary tumors. In the same line, numbers of LST were quite stable over passages in tumorgrafts, although some genomic changes were readily observed. A model that would account for these observations is that the instability induced by loss of *BRCA1* or *BRCA2* could be transient and compensated during tumor progression by various mechanisms (47–49).

Finally, our recognition of BRCAness with high sensitivity/specificity could have 2 major impacts in clinical management of breast cancer patients. Use of this genomic signature has an immediately translatable impact in identifying patients for whom a genetic test for *BRCA1/2* should be proposed. This may represent a major improvement especially in absence of family history of breast cancer, a situation found in as many as half of *BRCA1* mutation carriers (50). This recognition of BRCAness is inexpensive as compared with standard genetic testing, covers all possible mechanisms of *BRCA1* inactivation (germinal, somatic, or epigenetic), and results can be obtained in a timeframe compatible with therapeutic decisions. Thus, this signature could be of great interest with the emerging therapeutic perspective of exploiting HR defects by targeting complementary pathways (51). The efficiency of PARP inhibitors on *BRCA1/2* mutated breast cancers (52, 53) and the correlation of response to platinum salts with *BRCA1* status (12) strongly support the need to more accurately stratify sporadic BLC/TNBC according to actual BRCAness, which could easily be obtained using our genomic-based signature.

Disclosure of Potential Conflicts of Interest

A patent has been filed by Institut Curie based on the data presented in this report, with T. Popova, E. Manié, and M.-H. Stern as named inventors. No potential conflicts of interest were disclosed by the other authors.

Authors' Contributions

Conception and design: T. Popova, M.-H. Stern
Development of methodology: T. Popova
Acquisition of data (provided animals, acquired and managed patients, provided facilities, etc.): T. Popova, E. Manié, G. Rieunier, T. Dubois, O. Delattre, B. Sigal-Zafrani, M.A. Bollet, M. Longy, C. Houdayer, X. Sastre-Garau, A. Vincent-Salomon, D. Stoppa-Lyonnet
Analysis and interpretation of data (e.g., statistical analysis, biostatistics, computational analysis): T. Popova, E. Manié, G. Rieunier, C. Tirapo, A. Vincent-Salomon
Writing, review, and/or revision of the manuscript: T. Popova, E. Manié, G. Rieunier, T. Dubois, B. Sigal-Zafrani, M.A. Bollet, M. Longy, D. Stoppa-Lyonnet, M.-H. Stern
Administrative, technical, or material support (i.e., reporting or organizing data, constructing databases): T. Popova, E. Manié, V. Caux-Moncoutier, T. Dubois, O. Delattre, C. Houdayer
Study supervision: C. Houdayer, M.-H. Stern

Acknowledgments

The authors would like to thank Khadija Abidallah for technical support, Odette Mariani for managing tumor samples, Dr. Christophe Letourneau and Pr. Jean-Yves Pierga for careful reading, Dr. Jorge Reis-Filho for full access to NGS data, The Wellcome Trust Sanger Institute Cancer Genome Project for access to SNP-array data, Pr. Alexander Gorban for fruitful discussions, and Anthony Saul for English corrections.

Grant Support

Institut National de la Santé et de la Recherche Médicale, Cancéropole Ile-de-France, Institut Curie and its Translational Research Department. T. Popova is a recipient of a Fellowship from the Institut National Du Cancer (INCa)—GepiG. A. Vincent-Salomon is supported by a grant "Interface INSERM." This work is part of the "Canceropole Ile-de-France Hereditary Breast Cancer" program coordinated by D. Stoppa-Lyonnet and M.-H. Stern.

The costs of publication of this article were defrayed in part by the payment of page charges. This article must therefore be hereby marked *advertisement* in accordance with 18 U.S.C. Section 1734 solely to indicate this fact.

Received April 16, 2012; revised July 23, 2012; accepted August 6, 2012; published OnlineFirst August 29, 2012.

References

1. Rakha EA, Reis-Filho JS, Ellis IO. Basal-like breast cancer: a critical review. J Clin Oncol 2008;26:2568–81.
2. Foulkes WD, Stefansson IM, Chappuis PO, Begin LR, Goffin JR, Wong N, et al. Germline BRCA1 mutations and a basal epithelial phenotype in breast cancer. J Natl Cancer Inst 2003;95:1482–5.
3. Bergamaschi A, Kim YH, Wang P, Sorlie T, Hernandez-Boussard T, Lonning PE, et al. Distinct patterns of DNA copy number alteration are associated with different clinicopathological features and gene-expression subtypes of breast cancer. Genes Chromosomes Cancer 2006;45:1033–40.
4. Melchor L, Honrado E, Garcia MJ, Alvarez S, Palacios J, Osorio A, et al. Distinct genomic aberration patterns are found in familial breast cancer associated with different immunohistochemical subtypes. Oncogene 2008;27:3165–75.
5. Natrajan R, Weigelt B, Mackay A, Geyer FC, Grigoriadis A, Tan DS, et al. An integrative genomic and transcriptomic analysis reveals molecular pathways and networks regulated by copy number aberrations in basal-like, HER2 and luminal cancers. Breast Cancer Res Treat 2010;121:575–89.
6. Roy R, Chun J, Powell SN. BRCA1 and BRCA2: different roles in a common pathway of genome protection. Nat Rev Cancer 2012;12:68–78.
7. Turner N, Tutt A, Ashworth A. Hallmarks of 'BRCAness' in sporadic cancers. Nat Rev Cancer 2004;4:814–9.
8. Gonzalez-Angulo AM, Timms KM, Liu S, Chen H, Litton JK, Potter J, et al. Incidence and outcome of BRCA mutations in unselected patients with triple receptor-negative breast cancer. Clin Cancer Res 2011;17:1082–9.
9. Chin SF, Teschendorff AE, Marioni JC, Wang Y, Barbosa-Morais NL, Thorne NP, et al. High-resolution aCGH and expression profiling identifies a novel genomic subtype of ER negative breast cancer. Genome Biol 2007;8:R215.
10. Stefansson OA, Jonasson JG, Johannsson OT, Olafsdottir K, Steinarsdottir M, Valgeirsdottir S, et al. Genomic profiling of breast tumours in relation to BRCA abnormalities and phenotypes. Breast Cancer Res 2009;11:R47.
11. Joosse SA, Brandwijk KI, Mulder L, Wesseling J, Hannemann J, Nederlof PM. Genomic signature of BRCA1 deficiency in sporadic basal-like breast tumors. Genes Chromosomes Cancer 2011;50:71–81.
12. Silver DP, Richardson AL, Eklund AC, Wang ZC, Szallasi Z, Li Q, et al. Efficacy of neoadjuvant Cisplatin in triple-negative breast cancer. J Clin Oncol 2010;28:1145–53.
13. Vollebergh MA, Jonkers J, Linn SC. Genomic instability in breast and ovarian cancers: translation into clinical predictive biomarkers. Cell Mol Life Sci 2012;69:223–45.
14. Focken T, Steinemann D, Skawran B, Hofmann W, Ahrens P, Arnold N, et al. Human BRCA1-associated breast cancer: no increase in numerical chromosomal instability compared to sporadic tumors. Cytogenet Genome Res 2011;135:84–92.
15. Johannsdottir HK, Jonsson G, Johannesdottir G, Agnarsson BA, Eerola H, Arason A, et al. Chromosome 5 imbalance mapping in breast tumors from BRCA1 and BRCA2 mutation carriers and sporadic breast tumors. Int J Cancer 2006;119:1052–60.
16. Tirkkonen M, Johannsson O, Agnarsson BA, Olsson H, Ingvarsson S, Karhu R, et al. Distinct somatic genetic changes associated with tumor progression in carriers of BRCA1 and BRCA2 germ-line mutations. Cancer Res 1997;57:1222–7.
17. Wessels LF, van Welsem T, Hart AA, van't Veer LJ, Reinders MJ, Nederlof PM. Molecular classification of breast carcinomas by comparative genomic hybridization: a specific somatic genetic profile for BRCA1 tumors. Cancer Res 2002;62:7110–7.
18. Waddell N, Arnold J, Cocciardi S, da Silva L, Marsh A, Riley J, et al. Subtypes of familial breast tumours revealed by expression and copy number profiling. Breast Cancer Res Treat 2010;123:661–77.
19. Jonsson G, Staaf J, Vallon-Christersson J, Ringner M, Holm K, Hegardt C, et al. Genomic subtypes of breast cancer identified by array-comparative genomic hybridization display distinct molecular and clinical characteristics. Breast Cancer Res 2010;12:R42.
20. Joosse SA, van Beers EH, Tielen IH, Horlings H, Peterse JL, Hoogerbrugge N, et al. Prediction of BRCA1-association in hereditary non-BRCA1/2 breast carcinomas with array-CGH. Breast Cancer Res Treat 2009;116:479–89.
21. Lips EH, Mulder L, Hannemann J, Laddach N, Vrancken Peeters MT, van de Vijver MJ, et al. Indicators of homologous recombination deficiency in breast cancer and association with response to neoadjuvant chemotherapy. Ann Oncol 2011;22:870–6.
22. Vollebergh MA, Lips EH, Nederlof PM, Wessels LF, Schmidt MK, van Beers EH, et al. An aCGH classifier derived from BRCA1-mutated breast cancer and benefit of high-dose platinum-based chemotherapy in HER2-negative breast cancer patients. Ann Oncol 2011;22:1561–70.
23. Popova T, Manie E, Stoppa-Lyonnet D, Rigaill G, Barillot E, Stern MH. Genome Alteration Print (GAP): a tool to visualize and mine complex cancer genomic profiles obtained by SNP arrays. Genome Biol 2009;10:R128. Available from: http://bioinfo-out.curie.fr/projects/snp_gap/
24. Manie E, Vincent-Salomon A, Lehmann-Che J, Pierron G, Turpin E, Warcoin M, et al. High frequency of TP53 mutation in BRCA1 and sporadic basal-like carcinomas but not in BRCA1 luminal breast tumors. Cancer Res 2009;69:663–71.

Published OnlineFirst August 29, 2012; DOI: 10.1158/0008-5472.CAN-12-1470

25. Vincent-Salomon A, Gruel N, Lucchesi C, MacGrogan G, Dendale R, Sigal-Zafrani B, et al. Identification of typical medullary breast carcinoma as a genomic sub-group of basal-like carcinomas, a heterogeneous new molecular entity. Breast Cancer Res 2007; 9:R24.
26. Marty B, Maire V, Gravier E, Rigaill G, Vincent-Salomon A, Kappler M, et al. Frequent PTEN genomic alterations and activated phosphatidylinositol 3-kinase pathway in basal-like breast cancer cells. Breast Cancer Res 2008;10:R101.
27. Servant N, Bollet MA, Halfwerk H, Bleakley K, Kreike B, Jacob L, et al. Search for a gene-expression signature of breast cancer local recurrence in young women. Clin Cancer Res 2012;18:1704–15.
28. DeRose YS, Wang G, Lin YC, Bernard PS, Buys SS, Ebbert MT, et al. Tumor grafts derived from women with breast cancer authentically reflect tumor pathology, growth, metastasis and disease outcomes. Nat Med 2011;17:1514–20.
29. de Plater L, Lauge A, Guyader C, Poupon MF, Assayag F, de Cremoux P, et al. Establishment and characterisation of a new breast cancer xenograft obtained from a woman carrying a germline BRCA2 mutation. Br J Cancer 2010;103:1192–200.
30. Wellcome Trust Sanger Institute Cancer Genome Project. Available from: http://www.sanger.ac.uk/genetics/CGP
31. Stephens PJ, McBride DJ, Lin ML, Varela I, Pleasance ED, Simpson JT, et al. Complex landscapes of somatic rearrangement in human breast cancer genomes. Nature 2009;462:1005–10.
32. Elstrodt F, Hollestelle A, Nagel JH, Gorin M, Wasielewski M, van den Ouweland A, et al. BRCA1 mutation analysis of 41 human breast cancer cell lines reveals three new deleterious mutants. Cancer Res 2006;66:41–5.
33. Xu J, Huo D, Chen Y, Nwachukwu C, Collins C, Rowell J, et al. CpG island methylation affects accessibility of the proximal BRCA1 promoter to transcription factors. Breast Cancer Res Treat 2010;120: 593–601.
34. Forbes SA, Bindal N, Bamford S, Cole C, Kok CY, Beare D, et al. COSMIC: mining complete cancer genomes in the Catalogue of Somatic Mutations in Cancer. Nucleic Acids Res 2011;39:D945–50. Available from: http://www.sanger.ac.uk/genetics/CGP/cosmic/
35. Houdayer C, Moncoutier V, Champ J, Weber J, Viovy JL, Stoppa-Lyonnet D. Enhanced mismatch mutation analysis: simultaneous detection of point mutations and large scale rearrangements by capillary electrophoresis, application to BRCA1 and BRCA2. Methods Mol Biol 2010;653:147–80.
36. Natrajan R, Mackay A, Lambros MB, Weigelt B, Wilkerson PM, Manie E, et al. A whole-genome massively parallel sequencing analysis of BRCA1 mutant oestrogen receptor-negative and -positive breast cancers. J Pathol 2012;227:29–41.
37. Rasband WS. ImageJ, U.S. National Institutes of Health, Bethesda, MD, USA, 1997–2012. Available from: http://imagej.nih.gov/ij/
38. Staaf J, Vallon-Christersson J, Lindgren D, Juliusson G, Rosenquist R, Hoglund M, et al. Normalization of Illumina Infinium whole-genome SNP data improves copy number estimates and allelic intensity ratios. BMC Bioinformatics 2008;9:409.
39. Storchova Z, Kuffer C. The consequences of tetraploidy and aneuploidy. J Cell Sci 2008;121:3859–66.
40. Russnes HG, Vollan HK, Lingjaerde OC, Krasnitz A, Lundin P, Naume B, et al. Genomic architecture characterizes tumor progression paths and fate in breast cancer patients. Sci Transl Med 2010;2:38ra47.
41. Hicks J, Krasnitz A, Lakshmi B, Navin NE, Riggs M, Leibu E, et al. Novel patterns of genome rearrangement and their association with survival in breast cancer. Genome Res 2006;16:1465–79.
42. Stephens PJ, Greenman CD, Fu B, Yang F, Bignell GR, Mudie LJ, et al. Massive genomic rearrangement acquired in a single catastrophic event during cancer development. Cell 2011;144:27–40.
43. Mrasek K, Schoder C, Teichmann AC, Behr K, Franze B, Wilhelm K, et al. Global screening and extended nomenclature for 230 aphidicolin-inducible fragile sites, including 61 yet unreported ones. Int J Oncol 2010;36:929–40.
44. Van Loo P, Nordgard SH, Lingjaerde OC, Russnes HG, Rye IH, Sun W, et al. Allele-specific copy number analysis of tumors. Proc Natl Acad Sci U S A 2010;107:16910–5.
45. Pujana MA, Han JD, Starita LM, Stevens KN, Tewari M, Ahn JS, et al. Network modeling links breast cancer susceptibility and centrosome dysfunction. Nat Genet 2007;39:1338–49.
46. Fukasawa K. Centrosome amplification, chromosome instability and cancer development. Cancer Lett 2005;230:6–19.
47. Bouwman P, Aly A, Escandell JM, Pieterse M, Bartkova J, van der Gulden H, et al. 53BP1 loss rescues BRCA1 deficiency and is associated with triple-negative and BRCA-mutated breast cancers. Nat Struct Mol Biol 2010;17:688–95.
48. Feng Z, Scott SP, Bussen W, Sharma GG, Guo G, Pandita TK, et al. Rad52 inactivation is synthetically lethal with BRCA2 deficiency. Proc Natl Acad Sci U S A 2011;108:686–91.
49. Edwards SL, Brough R, Lord CJ, Natrajan R, Vatcheva R, Levine DA, et al. Resistance to therapy caused by intragenic deletion in BRCA2. Nature 2008;451:1111–5.
50. Moller P, Hagen AI, Apold J, Maehle L, Clark N, Fiane B, et al. Genetic epidemiology of BRCA mutations–family history detects less than 50% of the mutation carriers. Eur J Cancer 2007;43:1713–7.
51. Rehman FL, Lord CJ, Ashworth A. Synthetic lethal approaches to breast cancer therapy. Nat Rev Clin Oncol 2010;7:718–24.
52. Tutt A, Robson M, Garber JE, Domchek SM, Audeh MW, Weitzel JN, et al. Oral poly(ADP-ribose) polymerase inhibitor olaparib in patients with BRCA1 or BRCA2 mutations and advanced breast cancer: a proof-of-concept trial. Lancet 2010;376:235–44.
53. Kaye SB, Lubinski J, Matulonis U, Ang JE, Gourley C, Karlan BY, et al. Phase II, open-label, randomized, multicenter study comparing the efficacy and safety of olaparib, a poly (ADP-ribose) polymerase inhibitor, and pegylated liposomal doxorubicin in patients with BRCA1 or BRCA2 mutations and recurrent ovarian cancer. J Clin Oncol 2012; 30:372–9.

Published OnlineFirst August 29, 2012; DOI: 10.1158/0008-5472.CAN-12-1470

Cancer Research

Ploidy and Large-Scale Genomic Instability Consistently Identify Basal-like Breast Carcinomas with *BRCA1/2* Inactivation

Tatiana Popova, Elodie Manié, Guillaume Rieunier, et al.

Cancer Res 2012;72:5454-5462. Published OnlineFirst August 29, 2012.